ELSEVIER

NeuroImage

www.elsevier.com/locate/ynimg
NeuroImage xx (2008) xxx–xxx

Cerebral correlates of motor imagery of normal and precision gait

M. Bakker,[a,b] F.P. De Lange,[a] R.C. Helmich,[a,b] R. Scheeringa,[a] B.R. Bloem,[b,*] and I. Toni[a,c]

[a]*F.C. Donders Centre for Cognitive Neuroimaging, Radboud University Nijmegen, The Netherlands*
[b]*Department of Neurology, Radboud University Nijmegen Medical Centre, The Netherlands*
[c]*Nijmegen Institute for Cognition and Information, Radboud University, Nijmegen, The Netherlands*

Received 15 November 2007; revised 8 February 2008; accepted 10 March 2008

We have examined the cerebral structures involved in motor imagery of normal and precision gait (i.e., gait requiring precise foot placement and increased postural control). We recorded cerebral activity with functional magnetic resonance imaging while subjects imagined walking along paths of two different widths (broad, narrow) that required either normal gait, or exact foot placement and increased postural control. We used a matched visual imagery (VI) task to assess the motor specificity of the effects, and monitored task performance by recording imagery times, eye movements, and electromyography during scanning. In addition, we assessed the effector specificity of MI of gait by comparing our results with those of a previous study on MI of hand movements. We found that imagery times were longer for the narrow path during MI, but not during VI, suggesting that MI was sensitive to the constraints imposed by a narrow walking path. Moreover, MI of precision gait resulted in increased cerebral activity and effective connectivity within a network involving the superior parietal lobules, the dorsal precentral gyri, and the right middle occipital gyrus. Finally, the cerebral responses to MI of gait were contiguous to but spatially distinct from regions involved in MI of hand movements. These results emphasize the role of cortical structures outside primary motor regions in imagining locomotion movements when accurate foot positioning and increased postural control is required.

Keywords: Action simulation; Functional magnetic resonance imaging; Locomotion; Precision walking; Superior parietal lobule

Introduction

The neural control of locomotion is complex, requiring interactions between locomotor rhythm generation, balance control, and adaptation of the movements to motivational and environmental demands. Studies in cats and rodents have shown that while the production of the basic locomotor rhythm is largely dependent upon activity of central pattern generators within the spinal cord (Dietz, 2003; Grillner and Wallen, 1985), real-life gait also depends upon supra-spinal structures that are involved in adapting walking movements to environmental and motivational demands (Armstrong, 1988). In humans, little is known about the cerebral control of gait. Lesion studies have not been particularly informative, given that cerebral lesions causing higher-level gait disorders are typically multiple, or diffuse (Masdeu, 2001). Transcranial magnetic stimulation has provided electrophysiological evidence that the motor cortex is involved in the control of ankle muscles during walking (Petersen et al., 2001). Similarly, near-infrared spectroscopy has shown specific metabolic responses around the medial aspects of the central sulcus during actual gait (Miyai et al., 2001). In addition, single photon emission computed tomography studies have revealed that cerebral structures outside the primary motor cortex – such as the premotor cortex, parietal cortex, basal ganglia and cerebellum – are also contributing to gait (Fukuyama et al., 1997; Hanakawa et al., 1999). However, since these studies examined actual gait, they could not distinguish whether those effects were related to the feedforward control of gait or to changes in somatosensory feedback during gait. This issue is an instance of the general distinction that has been drawn between processes leading to the generation of a motor plan (that include predictions of the sensory consequences of the action), and processes related to the evaluation of sensory feedback (Blakemore and Sirigu, 2003; Grush, 2004; Wolpert et al., 1998). In this conceptual framework, it appears relevant to examine the cerebral structures specifically involved in the generation of the motor plan in the absence of sensory feedback due to movement execution. Here we have used motor imagery to address this issue. More specifically, given that precision gait (like passing a narrow door, or walking along uneven ground) relies on feedforward control more than normal gait (Hollands et al., 1995; Hollands and Marple-Horvat, 1996), we have examined the cerebral structures involved in motor imagery of both normal and precision gait.

Motor imagery, i.e. the mental simulation of an action without its actual execution (Jeannerod, 1994; Jeannerod, 2006), has been widely used to study the generation of a movement plan in the

* Corresponding author. University Medical Centre St Radboud, Department of Neurology (HP 935), PO Box 9101, 6500 HB Nijmegen, The Netherlands. Fax: +31 24 3541122.
E-mail address: b.bloem@neuro.umcn.nl (B.R. Bloem).
Available online on ScienceDirect (www.sciencedirect.com).

1053-8119/$ - see front matter © 2008 Elsevier Inc. All rights reserved.
doi:10.1016/j.neuroimage.2008.03.020

absence of sensory feedback (Lotze and Halsband, 2006). This approach relies on the notion that motor imagery involves the generation of a complete motor plan that is prevented from operating on the body (Grush, 2004; Jeannerod, 1994) (for a recent review of empirical support for this notion see Jeannerod, 2006). For instance, it has been shown that the current state of one's own body influences motor imagery performance (de Lange et al., 2006; Parsons, 1994; Shenton et al., 2004; Sirigu and Duhamel, 2001), and that motor imagery, motor preparation, and motor execution share cerebral and physiological correlates (Deiber et al., 1998; Lang et al., 1994; Porro et al., 1996; Roth et al., 1996; Stephan et al., 1995).

A few studies have already examined the cerebral structures involved in motor imagery of gait (Jahn et al., 2004; Jahn et al., 2008; Malouin et al., 2003; Miyai et al., 2001; Sacco et al., 2006), including motor imagery of precision gait (Malouin et al., 2003). More specifically, it was shown that when subjects imagine walking through a series of narrow passages their metabolism increases in the precuneus, the left supplementary motor area (SMA), the right inferior parietal cortex, and the left parahippocampal gyrus compared to when they imagine walking without any obstacles (Malouin et al., 2003). However, it remains unclear which of these cerebral structures is specifically involved in imagining precision gait, rather than spatial navigation, changes in walking direction, or visual imagery processes [see also Sacco et al., 2006]. In addition, these and other studies could not provide objective behavioural evidence that the subjects were specifically engaged in motor imagery of gait during the experiment. More generally, it is important to test whether the brain regions active during imagery of gait are part of a cerebral circuit dedicated to the control of gait, or whether imagery evokes general action plans that are not influenced by the specific effector involved in the action (Glover, 2004; Johnson et al., 2002). Imagery of flexion/extension of toes and fingers recruits separate precentral regions [Ehrsson et al., 2003, see also Stippich et al., 2002], and also imagery of more complex whole body and upper extremity movements reveals a homuncular organization in the primary sensorimotor cortices (Szameitat et al., 2007). However, it remains to be seen whether a similar homuncular somatotopic organization can be found outside the motor strip, and whether it is present for motor imagery of gait.

In this study, we have used a validated motor imagery protocol for examining the cerebral correlates of motor imagery of both normal and precision gait in humans (Bakker et al., 2007; Stevens, 2005). We asked subjects to imagine walking along visually presented paths of two different widths and five different distances that evoked either normal walking (broad path) or exact foot placement and increased postural control (narrow path). This manipulation allowed us to isolate behavioural and cerebral responses that were influenced by the different environmental constraints associated with imagining walking on supports of different size, distinguishing these responses from the generic effects associated with imagining walking along different distances. Furthermore, we assessed the motoric specificity of the cerebral and behavioural effects by using a matched visual imagery task, in which subjects imagined a disk moving along the same paths and distances used in the motor imagery tasks. Finally, we assessed the effector specificity of motor imagery of gait by comparing it with motor imagery of hand movements (de Lange et al., 2006).

Materials and methods

Subjects

Sixteen healthy men (age 22±2 years, mean±SD) participated after giving written informed consent according to the Declaration

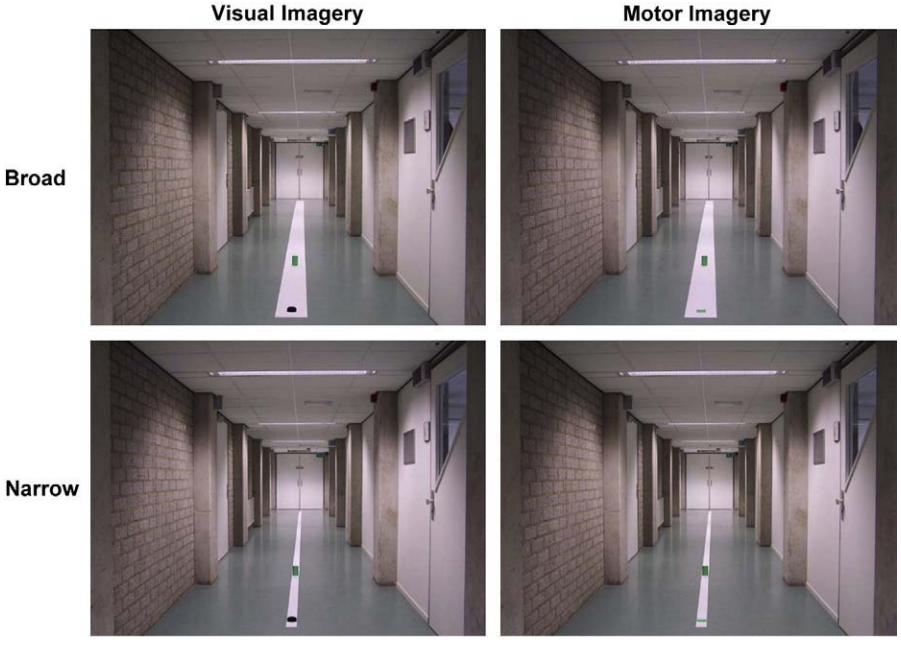

Fig. 1. Stimuli. Examples of photographs of walking trajectories presented to the subjects during the motor imagery (MI), and visual imagery (VI) experiment. The photos show a corridor with a white path in the middle and a green pillar positioned on the path. During MI trials, a green square is present at the beginning of the path. During VI trials, a black disc is present at the beginning of the path. During both tasks, the path width can be either broad (27 cm), or narrow (9 cm). In addition, the green pillar can be positioned at 2, 4, 6, 8 or 10 m from the green square or black disc (2 m in the photos presented in this figure). The figure is published in colour in the online version, but not in the printed version.

Please cite this article as: Bakker, M., et al., Cerebral correlates of motor imagery of normal and precision gait, NeuroImage (2008), doi:10.1016/j.neuroimage.2008.03.020

of Helsinki. All subjects had normal or corrected-to-normal vision, and no neurological or orthopaedic disturbances. All participants were consistent right-handers (Edinburgh Handedness Inventory (Oldfield, 1971) score 84±12%, mean±SD). The study was approved by the local ethics committee.

Experimental set-up

During the experiment, subjects were lying supine in the MR scanner. Head movements were minimized by an adjustable padded head holder. Visual stimuli were projected onto a screen at the back of the scanner and were seen through a mirror above the subjects' heads. The stimuli subtended a visual angle of ~10°. Stimuli presentation was controlled through a PC running Presentation software (Neurobehavioural systems, Albany, USA). Motor responses (i.e. right index finger flexions resulting in button presses) were recorded via an MR-compatible keypad (MRI Devices, Waukesha, WI), positioned on the right side of the subject's abdomen.

Stimuli

We used 20 photographs, each showing the same corridor with a path in the middle (path length = 12 m; thickness = 3 mm). There were narrow and broad paths (path width: 9 and 27 cm — see Fig. 1). The broad path allowed for walking over the path with a normal gait, whereas the narrow path required the subjects to carefully position their feet one in front of the other. At the near-end of the linoleum path there was either a green square (64 cm^2) or a black disc (diameter: 7.5 cm, width: 2.5 cm). Along the linoleum path there was a green pillar (diameter: 7.5 cm, width: 12 cm), placed at one of five different distances from the green square or the black disc (path length: 2, 4, 6, 8 and 10 m). This resulted in a total of 20 photographs (2 start markers × 5 path lengths × 2 path widths).

Tasks

Subjects performed two tasks: motor imagery (MI) and visual imagery (VI). Both tasks started with the presentation of one of the photographs described above, with the green square during MI trials, and the black disk during VI trials (Fig. 1). During MI, subjects were asked to imagine walking along the path shown in the photograph, starting from the green square and stopping at the green pillar. During VI, subjects were asked to imagine seeing the black disc moving along the path, from its starting position until the green pillar. During each trial, after a short inspection of the photograph on display, the subjects closed their eyes and imagined standing on the left side of the path, next to the green square (MI trials — Fig. 2) or the black disk (VI trials). The subjects pressed a button with the index finger of their right hand to signal that they had started imagining to step onto the path and walking along the path (MI trials), or imagining to see the disc moving along the path (VI trials). Subjects pressed the button again when they imagined that they had reached the end of the walking trajectory (MI trials), or that the disc had reached the end of the walking trajectory (VI trials). Following the second button press, a fixation cross was presented on the screen (inter-trial interval, ITI: 4–12 s), and the subjects could open their eyes. A transient change in size of the fixation cross announced the start of the next trial, i.e. the presentation of a new photograph of the corridor.

Experimental procedures

The MI and VI tasks were performed in two experimental sessions of 30 min each, separated by a break outside the scanner. Task order was counter-balanced across subjects. We have chosen a clustered task presentation to avoid the task-switching effects likely evoked by a trial-by-trial or block-by-block alternation between the two imagery tasks. We were concerned that task-switching might become especially problematic when the same experimental set-up would be used in follow-up studies on patient populations. An additional problem of a mixed task presentation is that the task instructions should be given at once for both tasks. This might make the task too complicated for some patient groups. For each session, the trial order was pseudo-randomized across the experimental factors [i.e., path width (2 levels) and path length (5 levels)].

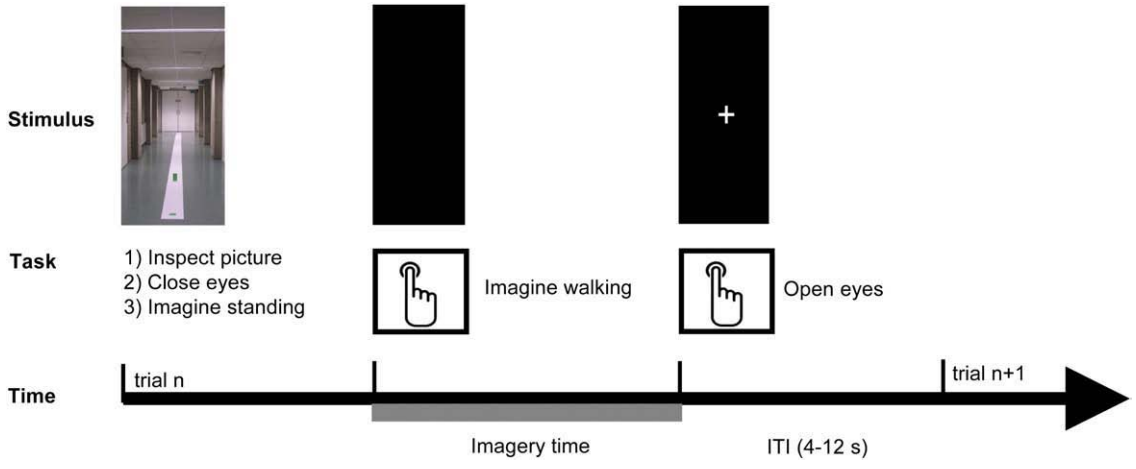

Fig. 2. Timecourse of motor imagery trials. During each trial, after a short inspection of the photo on display, the subjects closed their eyes and imagined standing on the left side of the path, next to the green square. The subjects pressed a button with the index finger of their right hand to signal that they had started imagining to step onto the path and walking along the path. The subjects pressed the button again when they imagined having reached the end of the walking trajectory. Following the second button press, a fixation cross was presented on the screen and the subjects could open their eyes. During the subsequent variable inter-trial interval (ITI, 4–12 s), a transient change in size of the fixation cross announced the start of the next trial, i.e. the presentation of a new photo of the corridor.

Please cite this article as: Bakker, M., et al., Cerebral correlates of motor imagery of normal and precision gait, NeuroImage (2008), doi:10.1016/j.neuroimage.2008.03.020

Before we started the experiment, subjects were familiarized with the actual paths and corridor, as shown in the photographs. The subjects were informed that, during the experiment, they would be shown photographs of these paths. They were then given written instructions for the first experimental session, followed by training in the relevant task, first outside the scanner (15 trials), and then inside the MR-scanner (7 trials). During the break between the first and second experimental session, the subjects were given written instructions for the second session, followed by training outside the MR-scanner until subjects felt confident they could perform the task (maximally 15 trials).

Prior to the MI task, subjects were asked to walk along short versions (three meters) of both the broad and the narrow linoleum paths (3 times for each path width), at a comfortable pace, avoiding to place their feet outside the path. We instructed subjects to pay attention to the feeling of walking along the different path widths, and to imagine walking in a similar way along the two different paths during the imagery trials. We instructed subjects to imagine the walking movement as vividly as possible, in a first person perspective, as if their legs were moving, but without making any actual movements. Prior to the VI task, subjects were familiarized with the actual black disc shown in the photographs, and they saw a video of the disc moving through the same corridor as in the photographs, but without a linoleum path in the middle of the corridor. The disc moved for 6 m, in a straight line, at a uniform speed of about 0.8 m/s. We instructed subjects to imagine seeing the disc moving in a similar way along the two different paths during the imagery trials. We instructed subjects to imagine seeing the disc moving as vividly as possible, without making any actual movements.

We recorded muscle activity of the legs during both sessions to control for overt muscle movements. To assess the reliability of this measure, we asked subjects (after the second session) to perform dorsiflexion movements of their right foot during MR acquisition at four different levels of contraction: no contraction (0%); minimal contraction (1%); half-maximal contraction (50%); maximal contraction (100%). Each contraction was triggered by the corresponding label (0%, 1%, 50%, 100%), and the subjects were asked to contract their muscle for as long as the label was presented on the screen. Each contraction lasted 10 s, followed by 30 s rest, and it was repeated two times in a semi-random order.

Data collection

MR images were acquired on a 3 T Trio MRI system (Siemens, Erlangen, Germany), using a standard circular polarized head coil for radio-frequency transmission and signal reception. Blood oxygenation level-dependent (BOLD) sensitive functional images were acquired using a single shot gradient EPI sequence (TR/TE=2360 ms/30 ms; 50 ms gap between successive volumes; 36 transversal slices; ascending acquisition; voxel size $3.5\times3.5\times3.0$ mm^3; FOV=224 mm^2). High-resolution anatomical images were acquired using an MP-RAGE sequence (TE/TR 3.93/2300 ms, 192 sagittal slices, voxel size $1.0\times1.0\times1.0$ mm^3, FOV 256 mm^2).

Muscle activity (EMG) was measured during task performance in the MR-scanner (MI, VI, and voluntary foot contractions) with a pair of carbon wired MRI compatible sintered silver/silver-chloride electrodes (Easycap, Herrsching-Breitbrunn, Germany), placed 3 cm apart along the muscle bellies of the right tibialis anterior. A neutral electrode was placed on the center of the patella. Following amplification and A/D conversion (Brain Products GmBH, Gilching, Germany), an optical cable fed the EMG signal to a dedicated PC outside the MR room for further off-line analysis (sampling rate: 5000 Hz). MR artefact correction followed the method described by (Allen et al., 2000; van Duinen et al., 2005), including low-pass filtering (400 Hz), and down-sampling (1000 Hz). Finally, we applied high-pass filtering (10 Hz, to remove possible movement artifacts), and rectification.

Eye movements were measured during task performance in the MR-scanner with a video-based infrared eyetracker (Sensomotoric Instruments, Berlin, Germany). Movements of the left eye were sampled at 50 Hz and fed to a dedicated PC outside the MR room for further off-line analysis.

Behavioural analysis and statistical inference

For each trial, we measured the time between the two button presses that marked the start and the end of the imagined visual or walking movements [imagery time (IT), see Fig. 2]. We excluded those few trials in which the subjects pressed the button only once, and therefore opened their eyes before the end of the IT, as revealed by online inspection of the eyetracker data. We investigated the effect of TASK (MI, VI), PATH WIDTH (narrow, broad), and PATH LENGTH (2, 4, 6, 8, 10 m) on IT. We also looked at effects of task ORDER (MI–VI, VI–MI) to investigate possible carry-over effects from one task to the next. The significance of the experimental factors was tested using a $2\times2\times5\times2$ repeated measures ANOVA. When interactions were significant, the simple main effects were investigated by additional repeated measures ANOVAs. The alpha-level of all behavioural analyses was set at $p<0.05$. Greenhouse–Geisser corrections were applied whenever the assumption of sphericity was not met, resulting in adjusted p-values based on adjusted degrees of freedom.

In addition, we examined whether IT obtained in each task conformed to Fitts' law (Fitts, 1954):

$$\mathrm{IT} = a + b\ \log_2(2{*}\mathrm{PATH\ LENGTH}/\mathrm{PATH\ WIDTH})$$

In the equation, a and b are constants. The term $\log_2(2*\mathrm{PATH\ LENGTH}/\mathrm{PATH\ WIDTH})$ is called the index of difficulty (ID). It describes the difficulty of the motor tasks. We calculated ID for each of our 10 experimental conditions [i.e., path width (2 levels) and path length (5 levels)]. The IT of conditions with the same ID value were averaged. Fitts' Law states that IT increases linearly with increasing ID. We examined how well IT conformed to Fitts' Law by calculating the linear regression of IT over ID for each task and for each subject separately. Finally, we examined whether the degree to which IT conformed to Fitts' Law was different for the different tasks, by considering the effect of task (MI, VI) on the variance in IT that could be explained by ID (r^2) after fisher's Z-score transformation using a paired sample t-test.

EMG analysis and statistical inference

For each trial of the imagery experiment, we considered the root mean square (rms) of the EMG signals measured during the IT (imagery epoch) and during the ITI (intertrial epoch — Fig. 2). For each subject, the average rms value of the EMG measured during the IT epoch was normalized to the average rms value of the ITI epoch, testing for an effect of TASK (MI, VI) with a paired samples t-test.

For the voluntary foot movement task, we considered the root mean square (rms) of the EMG signals measured during the 10 s

Please cite this article as: Bakker, M., et al., Cerebral correlates of motor imagery of normal and precision gait, NeuroImage (2008), doi:10.1016/j.neuroimage.2008.03.020

contraction (contraction epoch) and during the 20 s preceding the contraction (intertrial epoch). For each subject and for each of the four level of contraction (0%, 1%, 50%, 100%), the average rms value of the EMG measured during the contraction epoch was normalized to the average rms value of the intertrial epoch, testing for an effect of CONTRACTION (0%, 1%, 50%, 100%) with a repeated measures ANOVA and post-hoc paired sample *t*-tests.

fMRI analysis — preprocessing

Functional data were pre-processed and analyzed with SPM2 (Statistical Parametric Mapping, www.fil.ion.ucl.ac.uk/spm). The first four volumes of each participant's data set were discarded to allow for T1 equilibration. Afterwards, the image time series were spatially realigned using a sinc interpolation algorithm that estimates rigid body transformations (translations, rotations) by minimizing head-movements between each image and the reference image (Friston et al., 1995b). Subsequently, the time-series for each voxel was temporally realigned to the acquisition of the first slice. Images were normalized to a standard EPI template centered in MNI (Montreal Neurological Institute) space (Ashburner and Friston, 1997) by using linear transformations and resampled at an isotropic voxel size of 2 mm. The normalized images were smoothed with an isotropic 10 mm full-width-at-half-maximum Gaussian kernel. Anatomical images were spatially coregistered to the mean of the functional images (Ashburner and Friston, 1997) and spatially normalized by using the same transformation matrix applied to the functional images.

fMRI analysis — statistical inference (first level)

The ensuing pre-processed fMRI time series were analyzed on a subject-by-subject basis using an event-related approach in the context of the General Linear Model (Friston et al., 1995a). For each subject, regressors of interest were defined to characterize the cerebral response to imagery performed in each of the twenty different conditions of the 2 × 2 × 5 design [i.e., TASK (MI, VI), PATH WIDTH (narrow, broad) and PATH LENGTH (2, 4, 6, 8, 10 m)]. Other regressors of no interest modelled the cerebral response to picture inspection, button presses, and incorrect trials (i.e. those few trials in which the subjects pressed the button only once, and therefore opened their eyes before the end of the IT, as revealed by online inspection of the eyetracker data). Each effect was modelled on a trial-by-trial basis as a concatenation of square-wave functions convolved with a canonical haemodynamic response function, down-sampled at each scan, generating a total of 26 task-related regressors (Friston et al., 1998). For the regressors of interest, onsets of the square-wave functions were time-locked to the button press marking the onset of imagery, and durations corresponded to the mean IT across all imagery trials of the subject. For the picture inspection regressors, onsets were time locked to the onset of picture presentation, and offsets were time-locked to the button press marking the onset of imagery. For the button press regressor, onsets were time locked to the button press marking the offset of imagery, and duration was set at zero. For the incorrect trial regressor, onsets were time locked to the onset of picture presentation, and offsets were time-locked to the button press marking the offset of imagery. We also included 6 head motion regressors (describing translation and rotation in each of the three dimensions) and their temporal derivative, as derived from the spatial realignment procedure in the statistical model. Data were high-pass filtered (cutoff, 128 s) to remove low-frequency confounds such as scanner drifts. The statistical significance of the estimated evoked haemodynamic responses was assessed using *t*-statistics in the context of the General Linear Model. For each subject, we calculated contrasts of the parameter estimates for the effects of TASK and PATH WIDTH (i.e. MI-broad, MI-narrow, VI-broad, VI-narrow). We also considered linear parametric modulations of PATH LENGTH for each of these four effects (i.e. MI-broad-distance, MI-narrow-distance, VI-broad-distance, VI-narrow-distance), generating a total of eight contrasts for each subject.

fMRI analysis — statistical inference (second level)

The group-level random effects analysis modelled the experimental variance described by the eight contrasts for each subject by means of a one-way between-subjects analysis of variance (ANOVA), with non-sphericity correction. First, we considered the main effect of TASK (MI, VI). This refers to differential cerebral activity between the two tasks (MI > VI; VI > MI). Second, we looked for MI-specific effects of environmental constraints. This refers to differential cerebral activity evoked during MI between the two path widths (MI-broad > MI-narrow; MI-narrow > MI-broad). We were specifically interested in those regions that were specifically involved in MI, and increased their activity as a function of path width during MI, but not during VI. One way to fulfil these constrains while maintaining sensitivity is to mask the simple main effect (for instance, MI-narrow > MI-broad) with the main effect of task [i.e. MI > VI] and the relative interaction [i.e. (MI-narrow > MI-broad) > (VI-narrow > VI-broad); see also (Ramnani et al., 2001)]. In other words, when testing for the differential cerebral activity evoked during MI between the two path widths, we confined our search to regions showing a main effect of TASK (MI > VI) and a corresponding TASK × PATH WIDTH interaction [(MI-broad > MI-narrow) > (VI-broad > VI-narrow); (MI-narrow > MI-broad) > (VI-narrow > VI-broad)], using inclusive masking. An equivalent procedure was used to assess the effects of PATH WIDTH during VI. Third, we looked for MI-specific effects of imagined walking distance. This refers to cerebral activity that increased linearly as a function of PATH LENGTH during MI performance (MI-dist). We were again specifically interested in those regions that were involved in MI, and increased their activity as a function of path length during MI, but not during VI. Therefore, when testing for cerebral activity that increased linearly as a function of PATH LENGTH during MI performance, we confined our search to regions showing a main effect of TASK (MI > VI) and a corresponding TASK × PATH LENGTH interaction [(MI-dist > VI-dist)], using inclusive masking. An equivalent procedure was used to assess the effects of DISTANCE during VI. A list of the contrasts and functional masks used in this study is presented in Table 1. SPMs of the *t* statistic for these effects were created. We report the results of a random effects analysis, with inferences drawn at the voxel level, corrected for multiple comparisons across the whole brain using family-wise error (FWE) correction ($p < 0.05$).

Effective connectivity analysis

After having identified regions in the left and right superior parietal lobule (SPL) and the right middle occipital gyrus (MOG) that were specifically involved in motor imagery of gait along a narrow path, we performed a post-hoc analysis to explore which brain areas increased their couplings with these three regions

Please cite this article as: Bakker, M., et al., Cerebral correlates of motor imagery of normal and precision gait, NeuroImage (2008), doi:10.1016/j.neuroimage.2008.03.020

Table 1
Contrasts tested in the random effects analysis

Experimental factor	Contrasts	Functional (inclusive) masks
Task	MI>VI	
	VI>MI	
Path width	MI narrow>MI broad	a) MI>VI
		b) (MI narrow>MI broad)> (VI narrow>VI broad)
	MI broad>MI narrow	a) MI>VI
		b) (MI broad>MI narrow)> (VI broad>VI narrow)
	VI narrow>VI broad	a) VI>MI
		b) (VI narrow>VI broad)> (MI narrow>MI broad)
	VI broad>VI narrow	a) VI>MI
		b) (VI broad>VI narrow)> (MI broad>MI narrow)
Path length	MI distance	a) MI>VI
		b) MI distance>VI distance
	VI distance	a) VI>MI
		b) VI distance>MI distance

MI=motor imagery; VI=visual imagery.

during motor imagery of precision gait. To address this issue, we used the psychophysiological interaction (PPI) method described by (Friston et al., 1997). PPI analysis makes inferences about regionally specific responses caused by the interaction between the psychological factor and the physiological activity in a specified index area. We tested for differences in the regression slope of cerebral activity (on a voxel-by-voxel basis) on the basis of the activity in three source regions (e.g. left and right SPL, and right MOG, Fig. 5, Table 3), depending on the width of the path (broad or narrow) and the epoch of the motor imagery trial (picture presentation versus imagery). More specifically, the psychological factor was a vector coding for the interaction between the effect of path width during the motor imagery epoch, and the picture presentation epoch [i.e., (MI narrow>MI broad)>(Picture presentation narrow path>Picture presentation broad path)]. The source regions were defined by the first eigenvariate of the time series of all voxels within a 6 mm radius sphere centred on the regional maxima in the three source regions that showed a relative increase in BOLD signal during motor imagery of gait along a narrow compared to a broad path (MI-narrow>MI-broad; $p<0.5$ uncorrected). First, a PPI analysis for each subject and each source region was performed at the first level. Then, for each source region, individual PPI contrast images were entered into one-sample *t*-test at the second level. The statistical inference ($p<0.05$) was performed at the voxel-level, using FWE correction for multiple comparisons over a search volume defined by those voxels that were activated in the contrast MI>VI (as defined above).

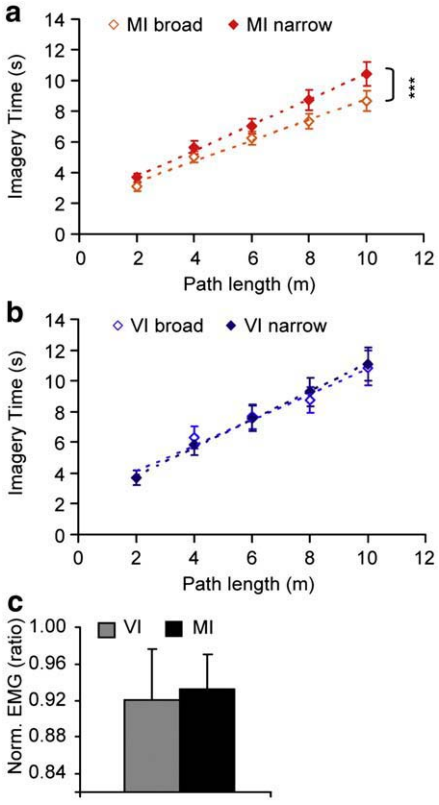

Fig. 3. Behavioural performance. Imagery times (IT) are shown for each of the five different path lengths (2, 4, 6, 8, and 10 m), and the two different path widths [Broad (27 cm), and Narrow (9 cm)], separately for each of the two tasks [a) motor imagery (MI), and b) visual imagery (VI)]. c) Averaged normalized electromyography (Norm. EMG) values measured during MI and VI trials, normalized to average intertrial interval EMG values on a subject by subject basis (imagery EMG/intertrial interval EMG). Data represent mean±SEM. ***$p<0.001$. The figure is published in colour in the online version, but not in the printed version.

fMRI analysis — anatomical inference

Anatomical details of significant signal changes were obtained by superimposing the SPMs on the structural images of the subjects. The atlas of (Duvernoy et al., 1991) was used to identify

Table 2
Stereotactic coordinates of the local maxima activated in the contrast "MI>VI"

Contrast	Anatomical label	Functional label	Hemisphere	*t*-value	*p*-value	*x*	*y*	*z*
MI>VI	Superior frontal gyrus	Dorsal premotor caudal	L	6.21	<0.001	−12	−10	68
	Superior frontal gyrus	Dorsal premotor caudal	R	5.00	0.013	16	−12	74
	Anterior cingulate gyrus	Rostral cingulate zone post	R	4.64	0.045	6	0	46
	Superior parietal lobule		R	5.50	0.002	20	−56	68
	Superior parietal lobule		L	4.60	0.051	−16	−58	60
	Putamen		L	5.01	0.012	−24	−4	8

Results are corrected for multiple comparisons across the whole brain (FWE, $p<0.05$). Stereotactic coordinates are reported in MNI (Montreal Neurological Institute) space. Details on the anatomical and functional labelling can be found in the Methods and Results sections.
L=left; MI=motor imagery; Post=Posterior; R=right; VI=visual imagery.

Please cite this article as: Bakker, M., et al., Cerebral correlates of motor imagery of normal and precision gait, NeuroImage (2008), doi:10.1016/j.neuroimage.2008.03.020

relevant anatomical landmarks. When applicable, Brodmann Areas were assigned on the basis of the SPM Anatomy Toolbox (Eickhoff et al., 2005), i.e., the anatomical position of our significant clusters and local maxima was formally tested against published three-dimensional probabilistic cytoarchitectonic maps. Finally, we compared our results with a previous study on motor imagery of hand movements (de Lange et al., 2006), to assess the relative anatomical location of the activated brain regions observed during MI of gait and during MI of hand rotations. More specifically, we compared the anatomical locations of our cerebral activity to that of cerebral areas showing increased cerebral activity with increasing biomechanical complexity during either left or right hand rotations, after using FWE correction to correct for multiple comparisons across the whole brain. Given that the whole brain analysis on MI of hand rotations did not reveal any suprathreshold cerebral activity in the putamen (whereas our whole brain analysis on MI of gait did), we also performed a dedicated VOI analysis in the putamen during MI of hand rotations using the Pick Atlas (Maldjian et al., 2003; Maldjian et al., 2004).

Results

Behavioural performance

There were no significant differences in imagery times between the two tasks (main effect of TASK: ($F(1,14)=2.9$, $p=0.1$). In both tasks, IT increased with increasing path length (main effect of PATH LENGTH: $F(1.1,15.6)=155.3$, $p<0.001$ — Figs. 3a,b). Crucially, the effect of path width on IT differed for the different tasks (TASK × PATH WIDTH interaction: $F(1,14)=39.5$, $p<0.001$). A smaller path width resulted in longer IT in the MI task ($F(1,14)=37.0$, $p<0.001$) (Fig. 3a), but had no effect on IT in the VI task ($F(1,14)=0.3$ $p=0.6$) (Fig. 3b). The TASK × PATH WIDTH interaction was influenced by the order in which the sessions were performed (TASK × PATH WIDTH × ORDER interaction: $F(1,14)=9.5$, $p<0.01$) (Supplementary Fig. 1). The interaction was stronger for the VI–MI order ($F(1,7)=43.0$, $p<0.001$), than for the MI–VI order ($F(1,7)=5.2$, $p=0.056$). This effect was related to a stronger effect of path width on IT during MI for the VI–MI order ($F(1,7)=32.8$, $p<0.01$), than for the MI–VI order ($F(1,7)=7.6$, $p<0.05$). These findings indicate that the crucial result of this study, i.e. the TASK × PATH WIDTH interaction, is present in both task orders, although larger in the VI–MI than in the MI–VI order. In other words, task order modulates the amplitude of the effect of path width on imagined walking, but not its presence. Finally, IT correlated linearly with ID in both tasks. Crucially, the variance in IT that could be explained by ID (r^2) was greater for MI (0.69 ± 0.03) than for VI (0.50 ± 0.01) (main effect of task: $F(1,15)=32.8$, $p<0.001$).

Muscular activity

We found no significant differences in EMG activity between the two tasks (main effect of TASK: ($F(1,15)=0.1$, $p=0.7$ — Fig. 3c). This result was unlikely to be due to lack of sensitivity, as we could find (in the same experimental setting) a significant effect of the amount of muscle contraction on EMG activity during voluntary contractions (main effect of CONTRACTION: $F(3,45)=45.4$, $p<0.001$), with significant differences between each of the four different levels of contraction (no contraction versus minimal contraction: $p<0.01$; minimal versus half-maximal contraction: $p<0.05$; half-maximal versus maximal contraction: $p<0.001$).

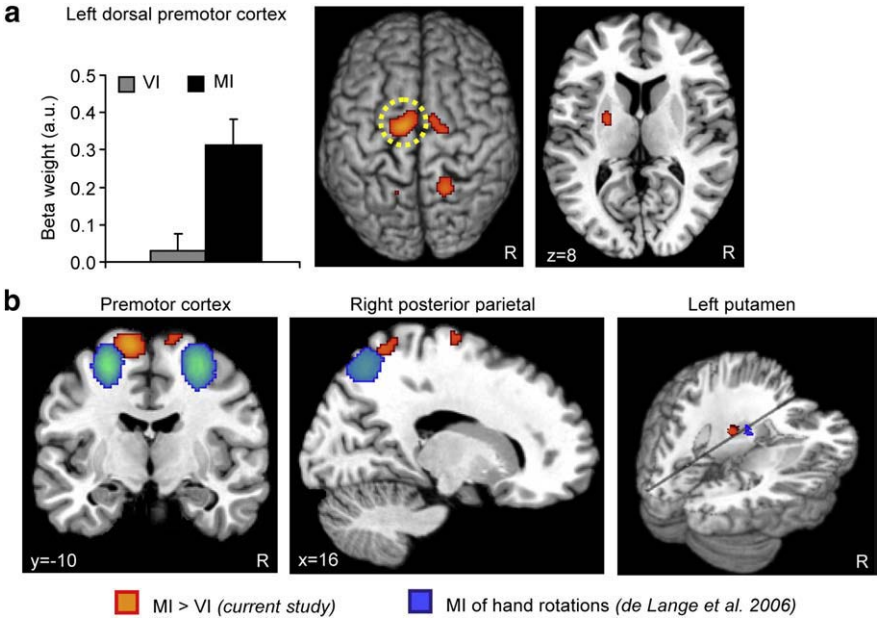

Fig. 4. Cerebral activity during motor imagery of gait. a) On the left, beta weights (mean ± sem) of the local maximum from left dorsal premotor cortex, separately for motor imagery (MI) and visual imagery (VI). On the right, statistical parametric map (SPM) of increased activity in the left putamen, in the right superior parietal lobule, and bilaterally in the dorsal premotor cortex during MI compared to VI [corrected for multiple comparisons ($p<0.05$) using family wise error (FWE)], superimposed on a rendered brain viewed from the top (middle panel), and on a transverse brain section (right panel). b) SPMs ($p<0.05$ FWE-corrected for multiple comparisons) of increased cerebral activity during MI of gait (compared to VI, in red-orange), and during MI of hand rotations (i.e. linear increase in activity with increasing stimulus rotation, in blue-cyan). R = right. The figure is published in colour in the online version, but not in the printed version.

Please cite this article as: Bakker, M., et al., Cerebral correlates of motor imagery of normal and precision gait, NeuroImage (2008), doi:10.1016/j.neuroimage.2008.03.020

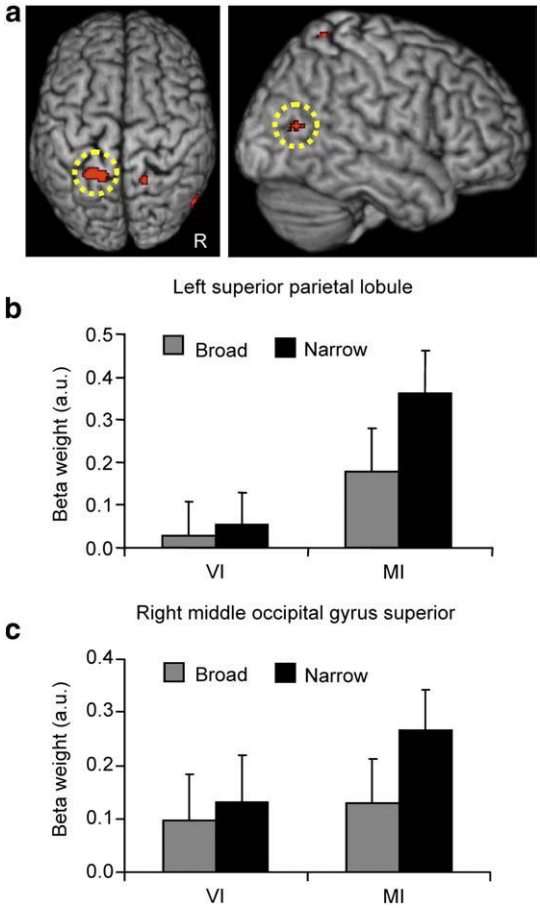

Fig. 5. Effect of path width on cerebral activity during motor imagery of gait. a) Statistical parametric map ($p<0.05$ FWE-corrected for multiple comparisons) showing increased cerebral activity in the left and right superior parietal lobule and in the right middle occipital gyrus during motor imagery (MI) along a narrow path (compared to MI along a broad path), superimposed on a rendered brain viewed from the top (left panel) and from the right (right panel). This simple main effect was searched within those voxels showing a TASK × PATH WIDTH interaction, i.e. stronger effects of path width during the MI task than during the VI task. b,c) Beta weights (mean ± sem) of the local maxima of the left superior parietal lobule and the right middle occipital gyrus for each of the two different path widths (broad, narrow), separately for MI and VI. R = right. The figure is published in colour in the online version, but not in the printed version.

Cerebral activity — task effects

We first identified cerebral regions showing differential activation during MI compared to VI (Fig. 4a, Table 2). Cerebral activity was greater during MI than VI in two clusters extending from the dorsal precentral sulcus to the superior frontal gyrus, bilaterally. Both clusters fell within BA6 (100%), but given the lack of cyto-architectonic studies on the border between lateral premotor cortex and supplementary motor area (SMA) proper in humans, it is difficult to draw precise inferences on the functional label of these superior frontal activations. A recent meta-analysis of functional imaging studies (Mayka et al., 2006) remains inconclusive, placing these activations at the border between the lateral premotor cortex and the SMA-proper. However, in macaques, as one moves from dorsal premotor cortex to SMA along a lateral-to-medial direction, the leg representation in dorsal premotor cortex is followed by the hand/arm representation in SMA, and then, more ventrally, by the leg representation in SMA (Luppino and Rizzolatti, 2000; Mitz and Wise, 1987). Crucially, the hand/arm representation in SMA partially extends on the lateral convexity, whereas the leg representation in SMA is located in the bank of the inter-hemispheric fissure. Under the assumption that our superior frontal activations are likely related to motor planning of the leg, and given that these activations are located exclusively in the dorsal convexity, we tentatively label them as dorsal premotor cortex caudal (PMdc) (Picard and Strick, 2001). The cingulate gyrus also showed increased neural activity during MI compared to VI. This cluster fell within the right BA6 (100%) (Eickhoff et al., 2005), and its local maximum can be functionally labelled as right rostral cingulate zone posterior (RCZp) (Picard and Strick, 1996). Furthermore, significant activation was found in the right SPL, and there was a marginally significant activation in the left SPL ($p=0.051$). Both parietal clusters fall caudal to BA2 (3% for right part, 0% for left part) (Eickhoff et al., 2005). Finally, significant activity was found in the left putamen. We also found a trend of increased cerebral activity in the right cerebellum ([36 −52 −34]; $t=4.46$, $p=0.079$, FWE).

In order to address the issue of a possible somatotopic organization of the MI-related activity found in the present study, we compared our results with those of a previous study on motor imagery of hand rotations (de Lange et al., 2006). The local maxima of both our left and right frontal clusters were located medially (12 and 14 mm, respectively) and dorsally (14 and 18 mm, respectively) from the local maxima of the corresponding frontal clusters activated during motor imagery of hand movements (Fig. 4b). There were no substantial differences in the rostro-caudal direction (2 mm). The local maxima of both our left and right parietal clusters were located rostrally (8 and 10 mm, respectively) and dorsally (12 and 16 mm, respectively) from the local maxima of the parietal clusters activated during motor imagery of hand movements (Fig. 4b). There were no substantial differences in the medio-lateral direction (2 and 0 mm, respectively). The local maximum of our left putamen activity was located laterally (6 mm), caudally (16 mm), and dorsally (10 mm) from the local maxima of the left putamen cluster activated during motor imagery of hand movements (Fig. 4b).

There were no areas that were more strongly activated during VI than during MI, i.e. VI was contained within MI.

Table 3
Stereotactic coordinates of the local maxima activated in the contrast "MI narrow > MI broad"

Contrast	Functional (inclusive) masks	Anatomical label	Hemisphere	*t*-value	*p*-value	*x*	*y*	*z*
MI nar > MI br	"MI > VI"	Superior parietal lobule	L	4.97	0.014	−16	−50	64
	&	Superior parietal lobule	R	4.88	0.019	16	−54	64
	"(MI nar > MI br) > (VI nar > VI br)"	Middle occipital gyrus superior	R	5.05	0.011	56	−70	12

Results are corrected for multiple comparisons across the whole brain (FWE, $p<0.05$). Stereotactic coordinates are reported in MNI (Montreal Neurological Institute) space. Details on the anatomical labelling can be found in the Methods and Results sections.
br = broad; L = left; MI = motor imagery; nar = narrow; R = right; VI = visual imagery.

Please cite this article as: Bakker, M., et al., Cerebral correlates of motor imagery of normal and precision gait, NeuroImage (2008), doi:10.1016/j.neuroimage.2008.03.020

Table 4
Stereotactic coordinates of the local maxima activated in the contrast "MI distance"

Contrast	Functional (inclusive) masks	Anatomical label	Functional label	Hemisphere	*t*-value	*p*-value	*x*	*y*	*z*
MI dist	"MI>VI"&	Superior frontal gyrus	SMA	L	6.21	<0.001	−6	−4	64
	"MI dist>VI dist"	Cerebellum (lobule VI)		R	5.55	0.002	40	−52	−26

Results are corrected for multiple comparisons across the whole brain (FWE, $p<0.05$). Stereotactic coordinates are reported in MNI (Montreal Neurological Institute) space. Details on the anatomical and functional labelling can be found in the Methods and Results sections.
dist=distance; L=left; MI=motor imagery; R=right; SMA=supplementary motor area; VI=visual imagery.

Cerebral activity — PATH WIDTH effects

We identified regions showing a differential effect of path width during MI compared to VI. We found increased activity in the left and right SPL during MI along a narrow compared to a broad path (Fig. 5, Table 3). Both clusters fell caudal to the probability range of BA2 (left: 9.2%, right: 0%) (Eickhoff et al., 2005), and it can be seen that in both regions cerebral activity increases with smaller path width during MI, but that cerebral activity is not influenced by path width during VI. We also found increased cerebral activity in the superior middle occipital gyrus (sMOG). The peak of this cluster was outside area V5/MT+(probability range: [0–10%]) (Eickhoff et al., 2005). When comparing the anatomical localization of sMOG to previous studies describing activity in the extrastriate body area (EBA), its respective displacement was 12 mm (Downing et al., 2001), 10 mm (Saxe et al., 2006) and 17 mm (Astafiev et al., 2004). Although there was no significant activation in the PMd or cerebellum at corrected threshold, trends were visible in both these areas at uncorrected threshold (left PMd [−26 −8 66]; $t=3.68$, $p<0.001$, uncorrected; left cerebellum [−40 −40 −32]; $t=3.42$, $p<0.001$, uncorrected).

We found no cerebral regions that decreased their activity with smaller path width during MI. There were also no cerebral regions that showed larger modulation by path width during the VI task than during MI. Finally, we found no regions that showed a TASK×PATH WIDTH interaction.

Cerebral activity — PATH LENGTH

Finally, we identified regions showing a differential effect of path length during MI compared to VI. We found that the superior frontal gyrus and right cerebellum increased their activity with increasing path length during MI (Table 4). The cluster in the superior frontal gyrus fell within the probability range (100%) of BA6 (Eickhoff et al., 2005), and its local maximum can be functionally labelled as SMA (Picard and Strick, 1996). The effect sizes show that cerebral activity increases with increasing path length during both MI and VI, but that the effect is greater for MI than for VI. We found no cerebral regions that showed larger modulation by path length during the VI task than during MI. Finally, we found no regions that showed a TASK×PATH LENGTH interaction.

Cerebral activity — effective connectivity

From the contrasts mentioned above, it appeared that the left and right SPLs and the right sMOG were specifically involved in motor imagery of gait along a narrow path (as compared to a broad path). We tested whether these regions contributed to motor imagery by examining whether its activity influenced the network supporting the motor imagery process (Fig. 4a). We found that the right sMOG increased its coupling as a function of path width with the right PMd ([16, −10, 72]; $t=4.52$; $p=0.012$, FWE corrected), and supplementary motor area ([−6, 0, 70]; $t=4.74$; $p=0.008$, FWE corrected). The right SPL increased its coupling as a function of path width with the left PMd ([−10, −4, 74]; $t=5.86$; $p=0.001$, FWE corrected).

Discussion

In this study we examined the cerebral structures involved in motor imagery of normal and precision gait. We distinguished imagery-related effects influenced by environmental constraints from generic imagery-related effects, and controlled for changes in muscle activity. We found that the activity and the inter-regional couplings between bilateral SPL, the dorsal precentral gyri, and the right sMOG were modulated by the degree of spatial accuracy of the imagined gait movements, with activity and connectivity increasing when subjects imagined walking along a narrow path requiring accurate positioning of each foot. These effects were specific to the MI task, resulting from a direct comparison with a matched visual imagery task. These effects were not related to differences in duration or number of steps between the two tasks, i.e. changes in path length did not influence cerebral activity in these regions during motor imagery of gait. These effects were embedded within a set of cerebral structures (PMd, RCZp, putamen, and cerebellum) with increased activity during motor imagery of gait, again compared to a matched visual imagery task. Furthermore, the parietal, premotor and putamen effects were contiguous but spatially distinct from activity evoked during motor imagery of hand movements (de Lange et al., 2006). These results indicate that in humans the precise spatial control of imagined gait relies on functional interactions between the SPL, the precentral gyrus, and the superior middle occipital gyrus. In the following sections, we discuss these findings and their relevance for current models of gait control.

Behavioural performance

The procedures used in this study were designed to isolate specific effects of first person kinesthetic motor imagery of gait, while excluding the presence of actual leg movements. We recorded EMG during task performance, showing that muscular activity during both MI and VI was matched (Fig. 3c). We recorded imagery times on a trial by trial basis, showing that IT increased as a function of path width during the MI trials, but not during the VI trials. This result indicates that motor imagery was sensitive to the environmental constraints imposed by a narrow walking path that allows only for positioning one foot at a time on the path. Furthermore, during motor imagery, there was an inverse and logarithmic relationship between movement difficulty and imagined movement time (Fitts, 1954).Visual imagery trials did not follow this rule of human movements. Finally, this task was adapted from a previous study showing that performance of motor imagery, but not visual imagery, was influenced by subjects' body posture (Stevens, 2005). Taken

Please cite this article as: Bakker, M., et al., Cerebral correlates of motor imagery of normal and precision gait, NeuroImage (2008), doi:10.1016/j.neuroimage.2008.03.020

together, these findings provide evidence that the subjects solved the task by using first person kinaesthetic imagery, without making any actual movement.

A distributed and dedicated circuit for motor imagery of gait

Motor imagery of gait resulted in increased cerebral activity bilaterally in the PMd, in the SPL, in the right RCZp, and in the left putamen. In addition, cerebral activity tended to be increased in the right cerebellum. These increases were relative to a matched visual imagery task, designed to control for unspecific effects (such as pressing a button, or general imagery-related effects). It should be noted that some of the cerebral effects we report might be related to imagined changes in the surrounding visual environment, given that during the visual imagery task subjects were instructed to see the black disc moving, while their own position remained fixed. These changes are likely to be part of the expected sensory consequences of the imagined movements, as will be discussed later. Furthermore, it might be argued that this comparison did not adequately control for accessory strategies, like counting, but it is unlikely that counting could account for the present results. Enumerating sequential foot movements modulates cerebral activity in the lateral premotor cortex (Kansaku et al., 2006), i.e. in locations that were considerably (>36 mm) lateral and ventral from the present effects.

It is possible that motor imagery relies on general action plans that are not effector-specific (Glover, 2004; Johnson et al., 2002), but our results suggest otherwise. We found that the cerebral responses to motor imagery of gait were contiguous to but spatially distinct from regions involved in motor imagery of hand movements. The somatotopic pattern described in this study fits with the findings of single-unit recordings in macaques, showing that in the premotor cortex the foot is represented in a location more medial and caudal than that of the hand (Godschalk et al., 1995; He et al., 1993; Kurata, 1989), whereas in the posterior parietal cortex the lower limb is rostral to the upper limb (Murray and Coulter, 1981). It remains to be seen how these findings can be reconciled with the opposite somatotopy found in single-subjects PET analyses of human parietal area 5 during actual arm and leg movements (Fink et al., 1997). Finally, in the putamen, cerebral activity during MI of gait was lateral, caudal, and dorsal to activity during MI of hand rotations. The dorsal and lateral location of foot relative to hand representations is in agreement with previous studies in humans (Gerardin et al., 2003; Lehericy et al., 1998; Maillard et al., 2000; Scholz et al., 2000), although the more caudal location of foot relative to hand is opposite to what has been reported before (Lehericy et al., 1998). Taken together, these findings suggest that motor imagery of gait activated cerebral structures that were specific for the effector used, although it remains to be seen whether the relative displacements of the results are consistent within subjects. It might be argued that the differences in spatial activation patterns between the MI of gait and MI of hand rotation may be attributable to differences in the reference frame of the movements. However, while it is generally accepted that different effectors are controlled by spatially separate portions of the primate precentral cortex (Graziano and Aflalo, 2007),it is less clear whether neurons encoding movements in different reference frames have such a clear spatial separation (Pesaran et al., 2006).

Over the precentral gyrus, activities evoked during MI of gait and during execution of right foot movement were spatially segregated (see Supplementary Fig. 2), a further indication that primary motor cortex is not specifically involved in motor imagery (de Lange et al., 2005).

We did not find any activity in brainstem structures during motor imagery of gait. Our study therefore does not confirm the finding by Jahn et al. (2008) that motor imagery of gait increases cerebral activity in several brainstem structures including the pedunculopontine nucleus (PPN). The PPN is a cerebral structure known to be specifically involved in gait control in quadrupeds (Garcia-Rill, 1991), but with a less precisely defined role in humans (Bussel et al., 1996; Calancie et al., 1994; Pahapill and Lozano, 2000). However, we cannot exclude that our study was simply not sensitive enough to detect changes in activity in the PPN, a small brainstem structure likely masked by pulsatile MR-artifacts.

Cerebral contributions to motor imagery of precision gait

Imagining to walk along a narrow path resulted in increased cerebral activity bilaterally in the superior parietal lobule and in the right sMOG, i.e. in structures with strong sensory afferences but without direct access to the spinal motor output. Given the role that the posterior parietal cortex plays in allocating attentional resources (Corbetta and Shulman, 2002), it might be argued that the increased SPL activity reflects differential visuo-spatial attention to the two walking paths, rather than environmental constraints on imagined gait. However, the parietal effect we report is unlikely to be driven by spatial attention per se: while spatial selective attention is known to modulate regions along the intraparietal sulcus (Corbetta and Shulman, 2002), the present effect was localized in the dorsomedial portion of the SPL. This region has been shown to incorporate proprioceptive information related to the current body position into the motor plan (de Lange et al., 2006), and to be involved in integrating visual and somatosensory information into the appropriate motor coordinates required for making spatially directed movements (Andersen, 1997; Wenderoth et al., 2006). Given that our task did not involve any actual movements, the observed activity cannot be related to the processing of visual and somatosensory feedback. However, following computational models based on engineering principles (Davidson and Wolpert, 2005), it has been proposed that both actual and imagined movements involve predictions of the sensory consequences of the action (Blakemore and Sirigu, 2003). During movement execution, the predicted sensory consequences are compared to the actual sensory feedback. During motor imagery, sensory predictions are generated in the absence of concurrent action production. The parietal lobe is thought to be involved in this process of the generation of sensory predictions (Blakemore and Sirigu, 2003; Wolpert et al., 1998). Given that precision gait relies more on feedforward control than normal gait (Hollands et al., 1995; Hollands and Marple-Horvat, 1996), we suggest that the SPL activity we observed might reflect predictions of the sensory (presumably, somatosensory) consequences of the motor plan. These predictions might take into account the width of the path, the position of the limb, and the intended walking movements. This interpretation also fits with our finding that, when a narrow path was presented, the right SPL increased its coupling with the PMd regions involved in motor imagery of gait. Crucially, our findings emphasize that these feedforward operations might become particularly relevant during precision gait. Finally, our finding is in agreement with the proposal based on cat studies that during precision walking the posterior parietal cortex is mainly involved in the planning, and the motor cortex is mainly involved in the execution of gait modifications (Drew et al., 2007).

Imagining walking along a narrow path also resulted in increased cerebral activity in the superior part of the right MOG, near the EBA

Please cite this article as: Bakker, M., et al., Cerebral correlates of motor imagery of normal and precision gait, NeuroImage (2008), doi:10.1016/j.neuroimage.2008.03.020

(Downing et al., 2001). This region has been implicated in the visual perception of human body parts (Downing et al., 2001), but our stimuli did not contain any body parts, and subjects had their eyes closed during imagery. We suggest that the enhanced sMOG activity during MI of walking along a narrow path reflects the generation of accurate predictions of the sensory (presumably visual) consequences of the motor plan. This interpretation fits with the finding that, when a narrow path was presented, the right sMOG increased its coupling with the premotor regions involved in motor imagery of gait. This increased coupling suggests that the sMOG activity might provide a relevant contribution to task performance, rather than being a by-product of collateral visual imagery in an allocentric perspective (Saxe et al., 2006). This interpretation implies that extrastriate regions might be involved in generating visual predictions relevant to motor control (Astafiev et al., 2004; Helmich et al., 2007; Toni et al., 2002). Given that during precision gait the subjects' gaze becomes directed downwards towards the area of footfall for each step (Hollands et al., 1995), it appears possible that during actual motor behaviour these putative visual predictions are matched against actual visual input, analogously to what has been reported in other sensory domains (Blakemore and Sirigu, 2003; Diedrichsen et al., 2005).

It might appear puzzling that an extrastriate area, rather than visually-responsive portions of the parietal cortex (like the inferior parietal lobule, IPL), is recruited for generating visual predictions of walking movements. It is possible that the IPL cannot support the control of a leg movement, given that this region lacks a clear leg representation (Rizzolatti and Luppino, 2001). Yet, other studies have demonstrated the generic involvement of this region in motor imagery of gait (Malouin et al., 2003; Sacco et al., 2006). A more likely possibility is that the contribution of the IPL to MI of gait reflects its role in processing goals of an action (Fogassi and Luppino, 2005; Hamilton and Grafton, 2006; Majdandzic et al., 2007). In our setting, imagining to walk along a narrow or a broad path requires different motor plans, but it entails the same goal ("reach the pillar"). Therefore, we speculate that the IPL supports the generation of sensorimotor predictions relative to the intended consequences of an action, whereas posterior extrastriate regions might support predictions more closely associated with the movement details.

Some cerebral regions might have been driven by the increased postural control required by gait, in particular along a narrow path. For instance, given that the cerebellum plays an important role in balance control (Morton and Bastian, 2004), that balance problems contribute to gait ataxia in patients with cerebellar lesions (Morton and Bastian, 2003), and that patients with cerebellar lesions have difficulties with tandem gait (Stolze et al., 2002), it is conceivable that the trend of increased activity observed in the cerebellum might be related to the balancing component during motor imagery of gait along the narrow path. Accordingly, some subjects mentioned (during a debriefing at the end of the experiment) to have put emphasis on balancing during motor imagery of gait along the narrow path. Unfortunately, we do not have a quantitative measure to determine the relevance of imagined balancing across our group, and the reduced strength of the cerebellar effect might be related to a between-subject inconsistency. Alternatively, the weak effect in the cerebellum might be related to the fact that the main role of the cerebellum in feedforward control is to make rapid predictions of the sensory consequences of motor actions, in order to compare them with the actual sensory consequences of a movement (Blakemore and Sirigu, 2003). Our imagery task did not involve any actual movements, and therefore the cerebellum may have only weakly been involved because it was not possible to compare the predictions to the actual sensory consequences.

Cerebral contributions to motor imagery of gait along different distances

We found that during motor imagery, cerebral activity in the cerebellum and SMA increased with increasing path length. Both these regions have been previously linked to timing functions (Halsband et al., 1993; Ivry, 1996; Rao et al., 1997). Therefore, it might be argued that activity in these regions is related to subjects estimating the time they would need to cover the indicated path. However, estimating the time required to cover the indicated path is required during both imagery tasks. We found no differences in IT between MI and VI, and therefore the VI task allowed us to correct for these time estimation effects. We suggest that the SMA and cerebellum are involved in a timing function that is specific for motor imagery of gait, such as the timing of the walking movements.

Conclusion

Our results show that motor imagery of gait results in increased activity in the PMd, RCZp, SPL, and putamen. In addition, the increased spatial accuracy required to imagine walking along a narrow path increases cerebral activity bilaterally in the SPL and in the right SMOG, together with increased effective connectivity between these regions and the dorsal premotor areas controlling foot movements. These results emphasize the role of cortical structures outside primary motor regions in imagining gait movements when accurate foot positioning is required. Given that gait impairments in neurological disorders like Parkinson's Disease become dramatically evident when patients need to negotiate environmental constraints (for example passing a narrow door) (Giladi et al., 1992), it becomes relevant to test whether these effects are related to altered responses and/or connectivity of the parietal, premotor, and extrastriate regions described in this study.

Acknowledgments

This research was supported by the Stichting Internationaal Parkinson Fonds (to MB and BB). BB was supported by the Netherlands Organisation for Scientific Research (NWO: VIDI grant no. 91776352). FdL and IT were supported by the Netherlands Organisation for Scientific Research (NWO: VIDI grant no. 45203339). RCH was supported by the Alkemade–Keuls foundation. We would like to thank Paul Gaalman for his expert assistance during scanning.

Appendix A. Supplementary data

Supplementary data associated with this article can be found, in the online version, at doi:10.1016/j.neuroimage.2008.03.020.

References

Allen, P.J., Josephs, O., Turner, R., 2000. A method for removing imaging artifact from continuous EEG recorded during functional MRI. NeuroImage 12, 230–239.

Andersen, R.A., 1997. Multimodal integration for the representation of space in the posterior parietal cortex. Philos. Trans. R. Soc. Lond., B Biol. Sci. 352, 1421–1428.

Armstrong, D.M., 1988. The supraspinal control of mammalian locomotion. J. Physiol. 405, 1–37.
Ashburner, J., Friston, K., 1997. Multimodal image coregistration and partitioning—a unified framework. NeuroImage 6, 209–217.
Astafiev, S.V., Stanley, C.M., Shulman, G.L., Corbetta, M., 2004. Extrastriate body area in human occipital cortex responds to the performance of motor actions. Nat. Neurosci. 7, 542–548.
Bakker, M., de Lange, F.P., Stevens, J.A., Toni, I., Bloem, B.R., 2007. Motor imagery of gait: a quantitative approach. Exp. Brain Res. 179, 497–504.
Blakemore, S.J., Sirigu, A., 2003. Action prediction in the cerebellum and in the parietal lobe. Exp. Brain Res. 153, 239–245.
Bussel, B., Roby-Brami, A., Neris, O.R., Yakovleff, A., 1996. Evidence for a spinal stepping generator in man. Paraplegia 34, 91–92.
Calancie, B., Needham-Shropshire, B., Jacobs, P., Willer, K., Zych, G., Green, B.A., 1994. Involuntary stepping after chronic spinal cord injury. Evidence for a central rhythm generator for locomotion in man. Brain 117 (Pt 5), 1143–1159.
Corbetta, M., Shulman, G.L., 2002. Control of goal-directed and stimulus-driven attention in the brain. Nat. Rev., Neurosci. 3, 201–215.
Davidson, P.R., Wolpert, D.M., 2005. Widespread access to predictive models in the motor system: a short review. J. Neural Eng. 2, S313–S319.
de Lange, F.P., Hagoort, P., Toni, I., 2005. Neural topography and content of movement representations. J. Cogn. Neurosci. 17, 97–112.
de Lange, F.P., Helmich, R.C., Toni, I., 2006. Posture influences motor imagery: an fMRI study. NeuroImage 33, 609–617.
Deiber, M.P., Ibanez, V., Honda, M., Sadato, N., Raman, R., Hallett, M., 1998. Cerebral processes related to visuomotor imagery and generation of simple finger movements studied with positron emission tomography. NeuroImage 7, 73–85.
Diedrichsen, J., Hashambhoy, Y., Rane, T., Shadmehr, R., 2005. Neural correlates of reach errors. J. Neurosci. 25, 9919–9931.
Dietz, V., 2003. Spinal cord pattern generators for locomotion. Clin. Neurophysiol. 114, 1379–1389.
Downing, P.E., Jiang, Y., Shuman, M., Kanwisher, N., 2001. A cortical area selective for visual processing of the human body. Science 293, 2470–2473.
Drew, T., Andujar, J.E., Lajoie, K., Yakovenko, S., 2007. Cortical mechanisms involved in visuomotor coordination during precision walking. Brain Res. Rev.
Duvernoy, H.M., Cabanis, E.A., Vannson, J.L., 1991. The human brain: surface, and three-dimensional sectional anatomy and MRI. Springer, Vienna.
Ehrsson, H.H., Geyer, S., Naito, E., 2003. Imagery of voluntary movement of fingers, toes, and tongue activates corresponding body-part-specific motor representations. J. Neurophysiol. 90, 3304–3316.
Eickhoff, S.B., Stephan, K.E., Mohlberg, H., Grefkes, C., Fink, G.R., Amunts, K., Zilles, K., 2005. A new SPM toolbox for combining probabilistic cytoarchitectonic maps and functional imaging data. NeuroImage 25, 1325–1335.
Fink, G.R., Frackowiak, R.S., Pietrzyk, U., Passingham, R.E., 1997. Multiple nonprimary motor areas in the human cortex. J. Neurophysiol. 77, 2164–2174.
Fitts, P.M., 1954. The information capacity of the human motor system in controlling the amplitude of movement. J. Exp. Psychol. 47, 381–391.
Fogassi, L., Luppino, G., 2005. Motor functions of the parietal lobe. Curr. Opin. Neurobiol. 15, 626–631.
Friston, K., Holmes, A.P., Worsley, K.J., Frith, C.D., Frackowiak, R.S., 1995a. Statistical parametric maps in functional imaging: A general linear approach. Hum. Brain Mapp. 2, 189–210.
Friston, K.J., Ashburner, J., Poline, J.B., Frith, C.D., Frackowiak, R.S., 1995b. Spatial registration and normalisation of images. Hum. Brain Mapp. 2, 165–189.
Friston, K.J., Buechel, C., Fink, G.R., Morris, J., Rolls, E., Dolan, R.J., 1997. Psychophysiological and modulatory interactions in neuroimaging. NeuroImage 6, 218–229.
Friston, K.J., Fletcher, P., Josephs, O., Holmes, A., Rugg, M.D., Turner, R., 1998. Event-related fMRI: characterizing differential responses. NeuroImage 7, 30–40.
Fukuyama, H., Ouchi, Y., Matsuzaki, S., Nagahama, Y., Yamauchi, H., Ogawa, M., Kimura, J., Shibasaki, H., 1997. Brain functional activity during gait in normal subjects: a SPECT study. Neurosci. Lett. 228, 183–186.
Garcia-Rill, E., 1991. The pedunculopontine nucleus. Prog. Neurobiol. 36, 363–389.
Gerardin, E., Lehericy, S., Pochon, J.B., Tezenas du, M.S., Mangin, J.F., Poupon, F., Agid, Y., Le Bihan, D., Marsault, C., 2003. Foot, hand, face and eye representation in the human striatum. Cereb. Cortex 13, 162–169.
Giladi, N., McMahon, D., Przedborski, S., Flaster, E., Guillory, S., Kostic, V., Fahn, S., 1992. Motor blocks in Parkinson's disease. Neurology 42, 333–339.
Glover, S., 2004. Separate visual representations in the planning and control of action. Behav. Brain Sci. 27, 3–24.
Godschalk, M., Mitz, A.R., van Duin, B., van der, B.H., 1995. Somatotopy of monkey premotor cortex examined with microstimulation. Neurosci. Res. 23, 269–279.
Graziano, M.S., Aflalo, T.N., 2007. Mapping behavioral repertoire onto the cortex. Neuron 56, 239–251.
Grillner, S., Wallen, P., 1985. Central pattern generators for locomotion, with special reference to vertebrates. Annu. Rev. Neurosci. 8, 233–261.
Grush, R., 2004. The emulation theory of representation: motor control, imagery, and perception. Behav. Brain Sci. 27, 377–396.
Halsband, U., Ito, N., Tanji, J., Freund, H.J., 1993. The role of premotor cortex and the supplementary motor area in the temporal control of movement in man. Brain 116 (Pt 1), 243–266.
Hamilton, A.F., Grafton, S.T., 2006. Goal representation in human anterior intraparietal sulcus. J. Neurosci. 26, 1133–1137.
Hanakawa, T., Fukuyama, H., Katsumi, Y., Honda, M., Shibasaki, H., 1999. Enhanced lateral premotor activity during paradoxical gait in Parkinson's disease. Ann. Neurol. 45, 329–336.
He, S.Q., Dum, R.P., Strick, P.L., 1993. Topographic organization of corticospinal projections from the frontal lobe: motor areas on the lateral surface of the hemisphere. J. Neurosci. 13, 952–980.
Helmich, R.C., de Lange, F.P., Bloem, B.R., Toni, I., 2007. Cerebral compensation during motor imagery in Parkinson's disease. Neuropsychologia 45, 2201–2215.
Hollands, M.A., Marple-Horvat, D.E., 1996. Visually guided stepping under conditions of step cycle-related denial of visual information. Exp. Brain Res. 109, 343–356.
Hollands, M.A., Marple-Horvat, D.E., Henkes, S., Rowan, A.K., 1995. Human eye movements during visually guided stepping. J. Mot. Behav. 27, 155–163.
Ivry, R.B., 1996. The representation of temporal information in perception and motor control. Curr. Opin. Neurobiol. 6, 851–857.
Jahn, K., Deutschlander, A., Stephan, T., Strupp, M., Wiesmann, M., Brandt, T., 2004. Brain activation patterns during imagined stance and locomotion in functional magnetic resonance imaging. NeuroImage 22, 1722–1731.
Jahn, K., Deutschlander, A., Stephan, T., Kalla, R., Wiesmann, M., Strupp, M., Brandt, T., 2008. Imaging human supraspinal locomotor centers in brainstem and cerebellum. Neuroimage 39, 786–792.
Jeannerod, M., 1994. The representing brain: neural correlates of motor intention and imagery. Behav. Brain Sci. 17, 187–245.
Jeannerod, M., 2006. Motor cognition: what actions tell the self. Oxford University Press, Oxford.
Johnson, S.H., Sprehn, G., Saykin, A.J., 2002. Intact motor imagery in chronic upper limb hemiplegics: evidence for activity-independent action representations. J. Cogn. Neurosci. 14, 841–852.
Kansaku, K., Johnson, A., Grillon, M.L., Garraux, G., Sadato, N., Hallett, M., 2006. Neural correlates of counting of sequential sensory and motor events in the human brain. NeuroImage 31, 649–660.
Kurata, K., 1989. Distribution of neurons with set- and movement-related activity before hand and foot movements in the premotor cortex of rhesus monkeys. Exp. Brain Res. 77, 245–256.
Lang, W., Petit, L., Hollinger, P., Pietrzyk, U., Tzourio, N., Mazoyer, B., Berthoz, A., 1994. A positron emission tomography study of oculomotor imagery. NeuroReport 5, 921–924.

Please cite this article as: Bakker, M., et al., Cerebral correlates of motor imagery of normal and precision gait, NeuroImage (2008), doi:10.1016/j.neuroimage.2008.03.020

Lehericy, S., van de Moortele, P.F., Lobel, E., Paradis, A.L., Vidailhet, M., Frouin, V., Neveu, P., Agid, Y., Marsault, C., Le Bihan, D., 1998. Somatotopical organization of striatal activation during finger and toe movement: a 3-T functional magnetic resonance imaging study. Ann. Neurol. 44, 398–404.

Lotze, M., Halsband, U., 2006. Motor imagery. J. Physiol. Paris 99, 386–395.

Luppino, G., Rizzolatti, G., 2000. The organization of the frontal motor cortex. News Physiol. Sci. 15, 219–224.

Maillard, L., Ishii, K., Bushara, K., Waldvogel, D., Schulman, A.E., Hallett, M., 2000. Mapping the basal ganglia: fMRI evidence for somatotopic representation of face, hand, and foot. Neurology 55, 377–383.

Majdandzic, J., Grol, M.J., Van Schie, H.T., Verhagen, L., Toni, I., Bekkering, H., 2007. The role of immediate and final goals in action planning: an fMRI study. NeuroImage 37, 589–598.

Maldjian, J.A., Laurienti, P.J., Kraft, R.A., Burdette, J.H., 2003. An automated method for neuroanatomic and cytoarchitectonic atlas-based interrogation of fMRI data sets. NeuroImage 19, 1233–1239.

Maldjian, J.A., Laurienti, P.J., Burdette, J.H., 2004. Precentral gyrus discrepancy in electronic versions of the Talairach atlas. NeuroImage 21, 450–455.

Malouin, F., Richards, C.L., Jackson, P.L., Dumas, F., Doyon, J., 2003. Brain activations during motor imagery of locomotor-related tasks: a PET study. Hum. Brain Mapp. 19, 47–62.

Masdeu, J.C., 2001. Neuroimaging and gait. Adv. Neurol. 87, 83–89.

Mayka, M.A., Corcos, D.M., Leurgans, S.E., Vaillancourt, D.E., 2006. Three-dimensional locations and boundaries of motor and premotor cortices as defined by functional brain imaging: a meta-analysis. Neuroimage 31, 1453–1474.

Mitz, A.R., Wise, S.P., 1987. The somatotopic organization of the supplementary motor area: intracortical microstimulation mapping. J. Neurosci. 7, 1010–1021.

Miyai, I., Tanabe, H.C., Sase, I., Eda, H., Oda, I., Konishi, I., Tsunazawa, Y., Suzuki, T., Yanagida, T., Kubota, K., 2001. Cortical mapping of gait in humans: a near-infrared spectroscopic topography study. NeuroImage 14, 1186–1192.

Morton, S.M., Bastian, A.J., 2003. Relative contributions of balance and voluntary leg-coordination deficits to cerebellar gait ataxia. J. Neurophysiol. 89, 1844–1856.

Morton, S.M., Bastian, A.J., 2004. Cerebellar control of balance and locomotion. Neuroscientist 10, 247–259.

Murray, E.A., Coulter, J.D., 1981. Organization of corticospinal neurons in the monkey. J. Comp. Neurol. 195, 339–365.

Oldfield, R.C., 1971. The assessment and analysis of handedness: the Edinburgh inventory. Neuropsychologia 9, 97–113.

Pahapill, P.A., Lozano, A.M., 2000. The pedunculopontine nucleus and Parkinson's disease. Brain 123 (Pt 9), 1767–1783.

Parsons, L.M., 1994. Temporal and kinematic properties of motor behavior reflected in mentally simulated action. J. Exp. Psychol. Hum. Percept. Perform. 20, 709–730.

Pesaran, B., Nelson, M.J., Andersen, R.A., 2006. Dorsal premotor neurons encode the relative position of the hand, eye, and goal during reach planning. Neuron 51, 125–134.

Petersen, N.T., Butler, J.E., Marchand-Pauvert, V., Fisher, R., Ledebt, A., Pyndt, H.S., Hansen, N.L., Nielsen, J.B., 2001. Suppression of EMG activity by transcranial magnetic stimulation in human subjects during walking. J. Physiol. 537, 651–656.

Picard, N., Strick, P.L., 1996. Motor areas of the medial wall: a review of their location and functional activation. Cereb. Cortex 6, 342–353.

Picard, N., Strick, P.L., 2001. Imaging the premotor areas. Curr. Opin. Neurobiol. 11, 663–672.

Porro, C.A., Francescato, M.P., Cettolo, V., Diamond, M.E., Baraldi, P., Zuiani, C., Bazzocchi, M., di Prampero, P.E., 1996. Primary motor and sensory cortex activation during motor performance and motor imagery: a functional magnetic resonance imaging study. J. Neurosci. 16, 7688–7698.

Ramnani, N., Toni, I., Passingham, R.E., Haggard, P., 2001. The cerebellum and parietal cortex play a specific role in coordination: a PET study. NeuroImage 14, 899–911.

Rao, S.M., Harrington, D.L., Haaland, K.Y., Bobholz, J.A., Cox, R.W., Binder, J.R., 1997. Distributed neural systems underlying the timing of movements. J. Neurosci. 17, 5528–5535.

Rizzolatti, G., Luppino, G., 2001. The cortical motor system. Neuron 31, 889–901.

Roth, M., Decety, J., Raybaudi, M., Massarelli, R., Delon-Martin, C., Segebarth, C., Morand, S., Gemignani, A., Decorps, M., Jeannerod, M., 1996. Possible involvement of primary motor cortex in mentally simulated movement: a functional magnetic resonance imaging study. NeuroReport 7, 1280–1284.

Sacco, K., Cauda, F., Cerliani, L., Mate, D., Duca, S., Geminiani, G.C., 2006. Motor imagery of walking following training in locomotor attention. The effect of "the tango lesson". NeuroImage 32, 1441–1449.

Saxe, R., Jamal, N., Powell, L., 2006. My body or yours? The effect of visual perspective on cortical body representations. Cereb. Cortex 16, 178–182.

Scholz, V.H., Flaherty, A.W., Kraft, E., Keltner, J.R., Kwong, K.K., Chen, Y.I., Rosen, B.R., Jenkins, B.G., 2000. Laterality, somatotopy and reproducibility of the basal ganglia and motor cortex during motor tasks. Brain Res. 879, 204–215.

Shenton, J.T., Schwoebel, J., Coslett, H.B., 2004. Mental motor imagery and the body schema: evidence for proprioceptive dominance. Neurosci. Lett. 370, 19–24.

Sirigu, A., Duhamel, J.R., 2001. Motor and visual imagery as two complementary but neurally dissociable mental processes. J. Cogn. Neurosci. 13, 910–919.

Stephan, K.M., Fink, G.R., Passingham, R.E., Silbersweig, D., Ceballos-Baumann, A.O., Frith, C.D., Frackowiak, R.S., 1995. Functional anatomy of the mental representation of upper extremity movements in healthy subjects. J. Neurophysiol. 73, 373–386.

Stevens, J.A., 2005. Interference effects demonstrate distinct roles for visual and motor imagery during the mental representation of human action. Cognition 95, 329–350.

Stippich, C., Ochmann, H., Sartor, K., 2002. Somatotopic mapping of the human primary sensorimotor cortex during motor imagery and motor execution by functional magnetic resonance imaging. Neurosci. Lett. 331, 50–54.

Stolze, H., Klebe, S., Petersen, G., Raethjen, J., Wenzelburger, R., Witt, K., Deuschl, G., 2002. Typical features of cerebellar ataxic gait. J. Neurol. Neurosurg. Psychiatry 73, 310–312.

Szameitat, A.J., Shen, S., Sterr, A., 2007. Motor imagery of complex everyday movements. An fMRI study. NeuroImage 34, 702–713.

Toni, I., Shah, N.J., Fink, G.R., Thoenissen, D., Passingham, R.E., Zilles, K., 2002. Multiple movement representations in the human brain: an event-related fMRI study. J. Cogn. Neurosci. 14, 769–784.

van Duinen, H., Zijdewind, I., Hoogduin, H., Maurits, N., 2005. Surface EMG measurements during fMRI at 3T: accurate EMG recordings after artifact correction. NeuroImage 27, 240–246.

Wenderoth, N., Toni, I., Bedeleem, S., Debaere, F., Swinnen, S.P., 2006. Information processing in human parieto-frontal circuits during goal-directed bimanual movements. NeuroImage 31, 264–278.

Wolpert, D.M., Goodbody, S.J., Husain, M., 1998. Maintaining internal representations: the role of the human superior parietal lobe. Nat. Neurosci. 1, 529–533.

Please cite this article as: Bakker, M., et al., Cerebral correlates of motor imagery of normal and precision gait, NeuroImage (2008), doi:10.1016/j.neuroimage.2008.03.020